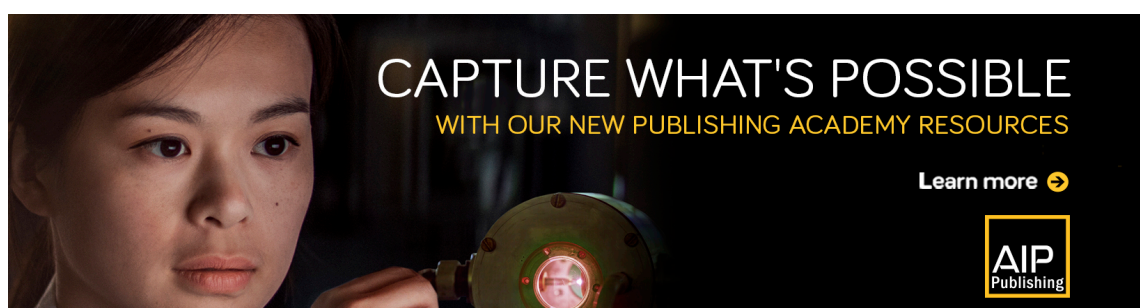# Symmetry and reversibility in mixing fluids

Eirik G. Flekko/y

View Online   Export Citation

Symmetry and reversibility in mixing fluids

Eirik G. Flekkøy[a)]

PMMH, Ecole Supérieure de Physique et de Chimie Industrielles, 10 rue Vauquelin, 75005 Paris, France

A notion of reversibility in miscible fluid flow, that does not depend on the amount of molecular diffusion, is introduced. This notion relies on a reciprocity relation for hydrodynamic dispersion which is derived and discussed. Using these results, an experimental technique for the measurement of hydrodynamic reversibility is investigated by means of numerical simulations employing a lattice Boltzmann model. Results demonstrate the sensitivity of the technique as well as potential biological applications. © *1997 American Institute of Physics.* [S1070-6631(97)04311-0]

I. INTRODUCTION

The irreversible spreading of a passive tracer by fluid flow and molecular diffusion is referred to as hydrodynamic dispersion. When a tracer pulse is injected into a system and then withdrawn, information on the interior structure of the system may be obtained from the return signal. Such experiments are called *echo* experiments.[1–3] In these experiments hydrodynamic and diffusive mechanisms of irreversibility work together in changing the tracer concentration profile, and the effect of the two can generally not be simply decomposed. Here a technique is introduced that, by a simple modification of the echo experiments, projects out the hydrodynamic contribution to the irreversibility, regardless of the amount of molecular diffusion that takes place. As a basis for this technique a reciprocity relation that resembles the Onsager symmetries of thermodynamics[4,5] is derived for dispersive systems.

The reciprocity relation states that in the case of dispersion on a *reversible* velocity field, the concentration measured at one point in the flow (called a receptor point) in response to a concentration pulse at another point in the flow (called the injection point) will be the same if the receptor and injection point are interchanged while simultaneously reversing the direction of the velocity field. This is the case regardless of the magnitude of the molecular diffusion. A reversible velocity field $\mathbf{u}(\mathbf{x})$ is one that simply changes sign everywhere, i.e., $\mathbf{u}(\mathbf{x}) \rightarrow -\mathbf{u}(\mathbf{x})$, when the external driving forces are reversed. While diffusion is always irreversible, hydrodynamics becomes irreversible only as the non-linear term in the Navier Stokes equations become significant.[6] This, however, happens in a wide regime of practical interest.[6] Using the reciprocity relation we can introduce a meaningful notion of reversibility even in the presence of significant molecular diffusion: The tracer transport between two points is simply considered reversible if the forward signal (corresponding to $\mathbf{u}$) and return signal (corresponding to $-\mathbf{u}$) are the same. The hydrodynamic irreversibility is then quantified as the deviation between the two signals.

A second point of interest is the fact that the reciprocity relation allows for the *prediction* of concentrations at any point $\mathbf{x}$ that can initially be made an independent source of

some kind of tracer. This technique, which will be described more thoroughly in the following, is illustrated by numerical simulations in Fig. 1, which shows dispersion in a random array of obstacles. It illustrates a two-step procedure. First a tracer pulse initialized in the injection point $\mathbf{x}_A$ is taken out by the left moving flow and the resulting concentration measured at receptor points located on the vertical line inside the system. Then the system is flushed, the flow direction is reversed and the receptor points made injection points. Figure 2 compares the resulting concentration measured at $\mathbf{x}_A$ with the prediction based on the measurements on points of the line. This technique may be of possible use in medical or biological applications—for instance it may allow for the prediction and placement of a desired amount of a medical preparation, say a cell poison, within some tissue of the body which is otherwise unaccessible. This could be within the lymph system or any closed cavity where a slow elastic expansion and contraction would drive a reversible flow.

Being an industrially important process the dispersing of a tracer in a porous geometry has received considerable attention over the last years.[7] While significant understanding of the dispersion effects caused by stagnation points,[1,7] boundary layers, dead ends end velocity differences between different flow channels (geometric dispersion), has been obtained, the understanding of dispersion effects of recirculation zones is less well developed. In studies of dispersion in rough fractures,[8] where recirculation zones are abundant, long time tails in the outgoing concentration profiles are observed as a result of the recirculation zones.[9,10] In general the reciprocity relation provides quantitative statements on the fact that regions which are hard to access by the action of hydrodynamic dispersion are correspondingly hard to leave. The present symmetry considerations thus appear to be useful in describing the trapping and release process that cause the significance of recirculation zones.[11]

II. RECIPROCITY RELATION

A. Proof from continuum theory

The evolution of a dispersing tracer concentration is described by the convection diffusion equation

[a)]Current address: Department of Physics, University of Oslo, P.O. Box 1048 Blindern, 0316 Oslo, Norway.

time = 0

time = 4096
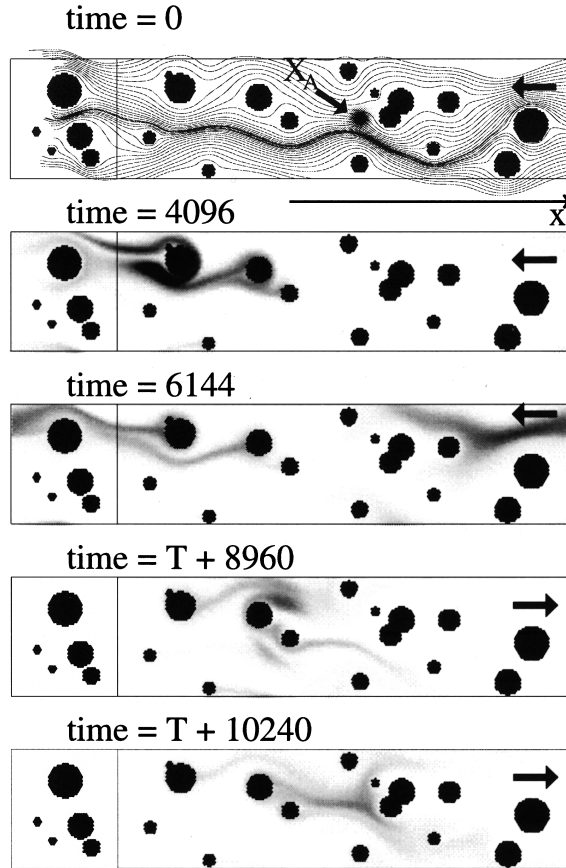
time = 6144

time = T + 8960

time = T + 10240

FIG. 1. The tracer concentration resulting from a point source at $\mathbf{x}_A$ (first 3 figures) and the injection at the vertical line (last 2 figures). The bold arrows show the direction of the flow, which is obtained from the Stokes equation (i.e. Re=0). Obstacles are shown in black. For each flow direction there is conservation of the tracer concentration which is shown in grey. The intensity of grey scale is exponential $g(C)=\exp(-\alpha C)$ ($g=1$ is white, $g=0$ is black) with $\alpha=40$ except in the first figure where $\alpha=4$. The streamlines shown in the first figure remain unchanged under flow reversal.
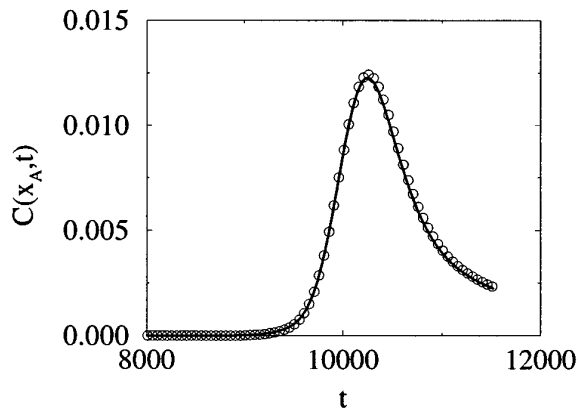

FIG. 2. The concentration $C(\mathbf{x}_A,t)$ in the simulation ($\bigcirc$) of Fig. 1 compared with the theoretical result (full line) given by Eq. (9). Here Re=0 and Pe=400.

$$\frac{\partial C_A}{\partial t} = -\nabla\cdot\mathbf{j}_A + m_0\delta(t)\delta(\mathbf{x}-\mathbf{x}_A), \qquad (1)$$

where the diffusive current $\mathbf{j}_A = -D\nabla C_A + \mathbf{u}\,C_A$, the tracer concentration $C_A(\mathbf{x},t)$ results from initializing the tracer mass m_0 in the fluid at the point $\mathbf{x}_A$, D is the molecular diffusivity and δ denotes Dirac's delta function. The replacement $A\to B$ must be accompanied by the replacement $\mathbf{u}(\mathbf{x})\to -\mathbf{u}(\mathbf{x})$ to describe the situation when the concentration is initialized in B.

The content of the present reciprocity relation might have been known in principle for some time, and it is certainly well established in the special case of vanishing flow velocity. However, the author has not yet seen a derivation of it for the case of a general flows. Therefore a short outline of the proof is given in the following:

Being a strictly macroscopic result the reciprocity relation can be derived directly from Eq. (1). To do this we take the time Fourier transform of Eq. (1) and multiply by the time Fourier transform of C_B. Since the flow is assumed reversible, the same equation with the replacements $A\to B$ and $\mathbf{u}\to -\mathbf{u}$ can be subtracted. A small manipulation then gives

$$0 = \nabla\cdot[\hat{C}_A\hat{\mathbf{j}}_B^- - \hat{C}_B\hat{\mathbf{j}}_A + \hat{C}_A\hat{C}_B\mathbf{u}] - \hat{C}_A\hat{C}_B\nabla\cdot\mathbf{u}$$
$$+ m_{A0}\hat{C}_B\delta(\mathbf{x}-\mathbf{x}_A) - m_{B0}\hat{C}_A\delta(\mathbf{x}-\mathbf{x}_B), \qquad (2)$$

where the $-$ superscript indicates that the reversed velocity field is used and the hat denotes the time Fourier transform. For incompressible flows ($\nabla\cdot\mathbf{u}=0$) in a materially closed system the first line of Eq. (2) vanishes upon volume integration. When the inverse Fourier transform is taken, Eq. (2) now directly implies the reciprocity relation

$$\frac{C_B(\mathbf{x}_A,t)}{m_{B0}} = \frac{C_A(\mathbf{x}_B,t)}{m_{A0}}, \qquad (3)$$

where m_{A0} (m_{B0}) is the tracer mass placed in $\mathbf{x}_A$ ($\mathbf{x}_B$). The above equation says that the concentration time signals obtained in $\mathbf{x}_A$ and $\mathbf{x}_B$ are the same when the concentrations are normalized by their initial values. Note that in order for hydrodynamic reversibility to hold, we *must* have $\nabla\cdot\mathbf{u}=0$. This follows since the steady compressible continuity equation $\nabla\cdot(\rho\mathbf{u})=\mathbf{u}\cdot\nabla\rho + \rho\nabla\cdot\mathbf{u}=0$ is only invariant under the replacement $\mathbf{u}\to -\mathbf{u}$. When $\nabla\rho\neq 0$, as will be the case in compressible flows, the equation is in general *not* invariant. This means that incompressibility is already implied by the requirement of reversibility, and does not enter as an additional requirement.

Analogous reciprocity relations are known to hold for electro-magnetic induction and in acoustic systems. In the case of acoustics it follows from the wave equation that a received sound signal is invariant under the exchange of the microphone and the sound source. It is also possible to employ the time reversal symmetry of the wave equation to *focus* a sound signal. Using an array of transducers, known as *time reversal mirrors*, that time invert, amplify and re-emit the received sound, Thomas *et al.* have focused ''echos'' of very large amplitudes.[12] This technique, how-

ever, relies on the time reversal symmetry of the wave equation. By contrast, Eq. (1) is not invariant under $t \rightarrow -t$.

B. Analogy to Onsager symmetries

The reciprocity relation of Eq. (3) can also be derived by considering a fluctuating concentration field and argue along the lines of irreversible thermodynamics.[11,13] This proof brings out the analogy between the present result and the famous thermodynamic Onsager symmetries.[4,5] If we view the system as a collection of microscopic, diffusing particles, the symmetry relation can be proved on the basis of the time reversibility of the microdynamics. For this purpose we introduce the (fluctuating) departure from the average tracer mass, $\Delta \widetilde{m}(\mathbf{x},t)$ inside a macroscopically small volume element Δv. We will assume that $\Delta \widetilde{m}$ gives the local fluctuation in the given particle population, which on the microscopic level is described by time reversible equations of motion. The particle motion thus described is superimposed on a mean drift velocity $\mathbf{u}(\mathbf{x})$. Time reversal invariance in this case means that if a motion picture showing all the particles moving according to the background field $\mathbf{u}(\mathbf{x})$, were shown backwards, it could not by means of statistical analysis be distinguished from a film with a background field $-\mathbf{u}(\mathbf{x})$, which was shown in the forward direction. Hence, under these conditions a time record of $\Delta \widetilde{m}(\mathbf{x},t)$ will be statistically invariant under a simultaneous reversal of $\mathbf{u}$ and the direction of time. This means that

$$\langle \Delta \widetilde{m}(\mathbf{x}_B,t)\Delta \widetilde{m}(\mathbf{x}_A,0)\rangle = \langle \Delta \widetilde{m}^-(\mathbf{x}_A,t)\Delta \widetilde{m}^-(\mathbf{x}_B,0)\rangle, \quad (4)$$

where the $-$ superscript indicates that the reversed velocity field is used, and where, in addition to time reversal invariance, time translational invariance of an equilibrium average has been used. We now make the key assumption of irreversible thermodynamics, that on the average spontaneous fluctuations decay according to the linear macroscopic laws,[13] in this case Eq. (1) with the identification

$$C(\mathbf{x},t) \rightarrow \langle \Delta \widetilde{m}(\mathbf{x},t)/\Delta v\rangle_{\widetilde{m}(\mathbf{x},0)} . \quad (5)$$

Here the average is taken over all mass distributions resulting from the given initial distribution $\widetilde{m}(\mathbf{x},0)$ after a given time t. Note that it is possible to split the average in Eq. (4) in two, first an average over all possible initial configurations $\widetilde{m}(\mathbf{x},0)$, and then an average over all possible outcomes of the initial configurations, i.e.,

$$\langle \Delta \widetilde{m}(\mathbf{x}_B,t)\Delta \widetilde{m}(\mathbf{x}_A,0)\rangle = \sum_{\widetilde{m}(\mathbf{x},0)} P[\widetilde{m}(\mathbf{x},0)]$$
$$\times \langle \Delta \widetilde{m}(\mathbf{x}_B,t)\Delta \widetilde{m}(\mathbf{x}_A,0)\rangle_{\widetilde{m}(\mathbf{x},0)}, \quad (6)$$

where $P[\widetilde{m}(\mathbf{x},0)]$ is the probability of having the initial state $\widetilde{m}(\mathbf{x},0)$. Now, since $\Delta \widetilde{m}(\mathbf{x}_A,0)$ factors outside the inner average in Eq. (6) the identification of Eq. (5) gives $\langle \Delta \widetilde{m}(\mathbf{x}_B,t)\Delta \widetilde{m}(\mathbf{x}_A,0)\rangle = \langle \Delta \widetilde{m}^2(\mathbf{x}_A,0)\rangle R(\mathbf{x}_B,\mathbf{x}_A,t)\Delta v$ where the response function R is given as $R = C_A(\mathbf{x}_B,t)/m_0$ where $C_A(\mathbf{x}_B,t) = \Delta m_A(\mathbf{x}_B,t)/\Delta v$ is given by Eq. (1). Equation (4) now directly implies the symmetry relation of Eq. (3). This

derivation is analogous to the derivation of the famous thermodynamic symmetry relations of Onsager[4,5] for which the principle of invariance of the microscopic equations of motion under the simultaneous reversal of time and the magnetic field $\mathbf{B}$, provides the theoretical basis. Here the velocity field plays the role of the magnetic field in the Onsager theory. The result is a symmetric response between the force of one quantity and the flux of another. Here the flux and the force are both signals of concentration, and the velocity $\mathbf{u}$ corresponds to the magnetic field $\mathbf{B}$.

III. SIMULATIONS

The simulations shown in Fig. 1 were carried out both to illustrate the sensitivity of the present technique to filter out small components of hydrodynamic irreversibility, and the ability to predict concentrations in *reversible* flows. The main purpose of these computations is not to simulate a particular experimental setup and provide a basis for quantitative comparison. It is rather to investigate the qualitative aspects of the physical ideas at hand. Therefore the particular geometry and the injection/receptor points are chosen rather arbitrarily. One particular part of the simulation design which may be unpractical is the whole line of receptor points. This would not be a practical necessity. However, it is done here in order to address yet another point, the possibility to use the information the reciprocity relation offers, to try and maximize the ratio of the concentration at $\mathbf{x}_A$ to the amount of tracer injected along the vertical line. The simulations mimic the time reversal mirrors of Thomas *et al.*[12] in the sense that they take a measured signal and time-invert it to produce a focusing effect. However, while the time-reversal mirrors only rely on the time-reversal symmetry of the wave equation, the present simulations rely on the reciprocity relation. Moreover, the time-reversal mirrors can in principle produce arbitrary sharp focusing while the present simulations will always produce a smeared result.

The solid obstacles are randomly distributed overlapping discs. They are chosen just to give a non-trivial, non-symmetric flow geometry containing stagnation points and slow flow zones. The simulations are carried out using a lattice Boltzmann model[14] that gives the solution $C(\mathbf{x},t)$ to Eq. (1) when the flow field is given by the steady Navier Stokes equations

$$\nabla \cdot \mathbf{u} = 0 \ , \quad (7)$$

$$G\rho\mathbf{u}\cdot\nabla\mathbf{u} = -\nabla p + \rho\nu\nabla^2\mathbf{u} + \mathbf{f}. \quad (8)$$

Here ρ is the mass density, p is the pressure, $\mathbf{f}$ an external force and ν the kinematic viscosity. The G-factor is an extra free parameter in the Boltzmann model.[15] By dividing Eq. (8) by G and absorbing it in the viscosity it is easily shown that a pertinent Reynolds number, which gives the ratio of inertial to viscous forces, has the form $\text{Re} = GU\overline{d}/\nu$ where ν is the kinematic viscosity, $\overline{d}$ the average obstacle diameter and U the average velocity. In Fig. 1 $\text{Re} = 0$ corresponding to the simulation of the Stokes equations (the flow is always steady).

A 64×256 lattice with periodic boundary conditions was used. The ratio of the characteristic diffusion time to the

Phys. Fluids, Vol. 9, No. 12, December 1997

Eirik G. Flekkøy   3597

advection time, the Péclet number Pe$= U\overline{d}/D$, was 400. The concentration at the receptor points on the line $x=$const is measured while the flow is moving leftwards. Consequently the response function $R(\mathbf{x}_i,\mathbf{x}_A,t) \equiv C(\mathbf{x}_i,t)/m_{A0}$, where the index i labels the lattice sites along the vertical line, is obtained. Afterwards, at $t=T$, the system is flushed, the flow is reversed and injection is performed along the line. In order to coordinate the return pulse at $\mathbf{x}_A$ the time of injection $t_I(\mathbf{x}_i)$ is chosen by the first-in-last-out rule $t_I(\mathbf{x}_i)=T-t_M(\mathbf{x}_i)$, where $t_M(\mathbf{x}_i)$ is the maximum point of $C(\mathbf{x}_i,t)$. The injected tracer mass at every point $\mathbf{x}_i$ was chosen as $m(\mathbf{x}_i)=aC(\mathbf{x}_i,t_M(\mathbf{x}_i))$ so that high concentrations only occur in regions where they have a strong effect. In the simulations the prefactor a can have any value and was chosen so that the maximum concentration along the line $x=$const was 0.1(lattice unit)$^{-2}$. Time is measured in units of the discrete updating step of the simulation and space in units of the lattice constant. The concentration in $\mathbf{x}_A$ resulting from the injection along the line, can be written

$$C_{\text{th}}(\mathbf{x}_A,t)=\sum_i R(\mathbf{x}_i,\mathbf{x}_A,t-t_I(\mathbf{x}_i))m(\mathbf{x}_i),\qquad(9)$$

where the reciprocity relation has been used to replace $R(\mathbf{x}_A,\mathbf{x}_i,t)$ by $R(\mathbf{x}_i,\mathbf{x}_A,t)$.

Figure 2 shows the measured and predicted values of the concentration $C(\mathbf{x}_A,t)$. The agreement is seen to be excellent. It was checked that when tracer was injected at the $\mathbf{x}_i$'s at a constant rate, 3 orders of magnitude more tracer mass was required in order to produce approximately the same maximum concentration at $\mathbf{x}_A$ as shown in Figs. 1 and 2, in the same period of time. The peak concentration in Fig. 2 can be made significantly higher by changing $\mathbf{x}_A$ or the direction of the externally imposed flow. The maximum value of $C(\mathbf{x}_A,t)$ could be increased by a factor of 10 by shifting $\mathbf{x}_A$ a bit downwards. While the sharpness of the peak and the small ratio between the injected tracer mass and the maximum value of $C(\mathbf{x}_A,t)$ depends on the particular injection procedure chosen here, the agreement between the predicted and measured concentrations seen in Fig. 2, does not. Hence, Eq. (9) may be used as a means to optimize the injection procedure (choice of injection points and the magnitude of the injected mass), for instance to obtain a sharply defined concentration at $\mathbf{x}_A$.

Generally, a tracer that is moving in a flow with velocity gradients will disperse in a way that produces a linear increase with time of the second moment of the concentration field, just as simple diffusion. By contrast, Fig. 3 shows that mean the square of the tracer x-position (around its average), $\Delta x^2=\langle x^2\rangle-\langle x\rangle^2$, where the average is defined by $\langle x\rangle=\int d^2x\,xC(\mathbf{x},t)/\int d^2x\,C(\mathbf{x},t)$. Initially ΔX^2 decreases with time, illustrates how the re-injection procedure described above creates a focusing of the signal. In contrast, for a random initialization of the tracer, $\langle X^2\rangle-\langle X\rangle^2$ would on the average increase linearly with time. This is still expected to happen in the long time limit in the present case, as eventually there will be a crossover to normal dispersion.

From a practical point of view a main problem is to make the focusing point $\mathbf{x}_A$ an initial source of tracer. How
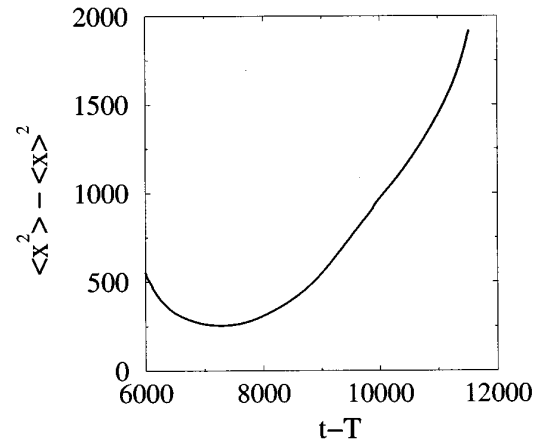

FIG. 3. The mean square spread of the tracer concentration after re-injection. The graph corresponds to the simulation of Fig. 1.

this can be achieved depends on the particular system at hand. In the case of biological systems it may be possible to solve the problem with the aid of *caged compounds*.[16] Caged compounds are substances that in the matter of milliseconds can be photo activated by ultra violet light to release biologically active or passive tracers. Such caged compounds can be coupled to appropriate antibodies to have them attach to different biological material (cells). Since light may be directed very precisely, for instance through the optics of a microscope, the tracer may then be released with high accuracy both in time and space. Hence, if $\mathbf{x}_A$ denotes the position of some particular tissue that can be identified by appropriate antibodies, caged compounds can be used for the messenger substance that is to be released at $\mathbf{x}_A$. One can also imagine substances that are sensitive to pressure and able to release a detectable tracer signal when subjected to a sudden punch, and there might be cases where an electric current through the system has the desired effect. If there is an array of probes over a cross section of the flow, the amount of tracer released at $\mathbf{x}_A$ can be measured by integration of the outside signal.

The tracer signal which is taken out of the sample may be different in chemical composition from the tracer that is injected. Different diffusivities, say D_1 and D_2, may be compensated for by taking the initial flow velocity to be a fraction (D_1/D_2) of the return velocity in order to have the same Péclet number of the in and out moving flows. This will render Eq. (9) valid. For experimental testing of the technique, were non-invasive initialization of the concentration at $\mathbf{x}_A$ may not be an issue, there exists electro-chemical experiments where the probe can be used both for the initial injection at $\mathbf{x}_A$, the measurements and the re-injection of tracer.[2]

When $G=0$, or equivalently when the non-linear term in Eq. (8) can be neglected, Eq. (8) is invariant under the replacements $\mathbf{u}\to-\mathbf{u}$, $\mathbf{f}\to-\mathbf{f}$ and $\nabla P\to-\nabla P$. When $G\neq0$ this symmetry is broken. Physically this means that because of fluid inertia, streamlines start to depend on the flow direction. Hence, since Eq. (9) holds only for reversible
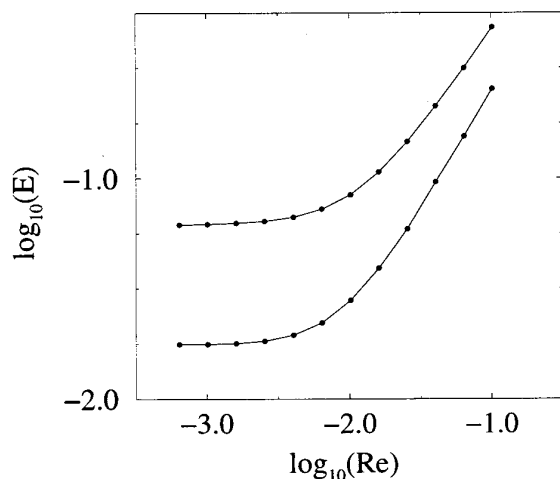
Eirik G. Flekkøy

FIG. 4. The integrated difference between the predicted and measured values of $C_A(t)$, E, as a function of the Reynolds number. The upper curve corresponds to the case where $\mathbf{x}_A$ is in region of strong flow, whereas the lower curve corresponds to the case where $\mathbf{x}_A$ is in a sheltered region of low flow velocity.

flows, it can be used to measure the magnitude of the hydrodynamic irreversibiliy. The quantity we define for this purpose is the relative deviation E between the prediction of Eq. (9) and the measured signal:

$$E^2 = \frac{1}{T} \int dt [(C_{\mathrm{th}}(\mathbf{x}_A,t) - C(\mathbf{x}_A,t))/C(\mathbf{x}_A,t)]^2. \quad (10)$$

Here T is the length of the time integration domain.

Figure 4 shows E resulting from a series of simulations like those in Fig. 1, but with varying Reynolds numbers (obtained by varying G, keeping U and ν fixed). Already at $\mathrm{Re} \geqslant 10^{-2}$, where Re is still defined by the average disc diameter, inertial effects become significant compared to the other error sources, thus demonstrating the sensitivity of the method. Comparable results where observed in Ref. 6 where great care had to be taken to minimize the effect of molecular diffusion at low values of Re. In the present case the molecular diffusion simply does not enter as a noise factor. Figure 4 shows that even at $\mathrm{Re} < 10^{-3}$ the value of E increases to 7% when $\mathbf{x}_A$ is placed in the mainstream of the flow. This is most likely due to the fact that the time between injection and arrival at $\mathbf{x}_A$ is decreased and the discretization errors caused by a finite injection time and a finite initial concentration spread at $\mathbf{x}_A$, is increased.

IV. CONCLUSION

In conclusion a general reciprocity relation for low Reynolds number hydrodynamic dispersion has been derived and applied to design a general method for the detection of irreversibility in low Reynolds number flows. It has also been used to predict the concentration signal that results from outside injection into a system. It has been speculated and argued that this technique may have interesting medical, biological and industrial applications. If two mutually reactive fluids are made to meet inside the medium, the technique could perhaps be used to control focused chemical reactions, for instance to remove local impurities.

Among the many interesting questions that could be addressed experimentally is to what extent the prediction of Eq. (9) will hold when the flow penetrates a complex 3D geometry, say a porous media with many pore lengths separating $\mathbf{x}_A$ and the reinjection points.

[1] U. Oxaal, E. G. Flekkøy, and J. Feder, ''Irreversible dispersion at a stagnation point: Experiments and lattice boltzmann simulations,'' Phys. Rev. Lett. **72**, 3514 (1994).
[2] P. Rigord, A. Calvo, and J. P. Hulin, ''Transition to irreversibility for the dispersion of a tracer in a porous media,'' Phys. Fluids A **2**, 681 (1990).
[3] J. P. Hulin and T. J. Plona, ''Echo tracer dispersion in porous media,'' Phys. Fluids A **1**, 1341 (1989).
[4] L. Onsager, ''Reciprocal relations in irreversible processes i,'' Phys. Rev. **37**, 405 (1931).
[5] L. Onsager, ''Reciprocal relations in irreversible processes ii,'' Phys. Rev. **38**, 2265 (1931).
[6] E. G. Flekkøy, T. Rage, U. Oxaal, and J. Feder, ''Hydrodynamic irreversibility in creeping flow,'' Phys. Rev. Lett. **77**, 4170 (1996).
[7] *Disorder and Mixing*, edited by E. Guyon, J.-P. Nadal, and Y. Pomeau (Kluwer Academic, Dordrecht/Boston/London, 1988).
[8] I. Ippolito, G. Daccord, E. J. Hinch, and J. P. Hulin, ''Echo tracer dispersion in model fractures with a rectangular geometry,'' J. Cont. Hydr. **16**, 87 (1994).
[9] J. Koplik, I. Ippolito, and J. P. Hulin, ''Tracer dispersion in rough channels: A two-dimensional numerical study,'' Phys. Fluids A **5**, 1333 (1993).
[10] E. Guyon, Y. Pomeau, J. P. Hulin, and C. Baudet, ''Dispersion in the presence of recirculation zones,'' Nucl. Phys. B **2**, 174 (1987).
[11] E. G. Flekkøy (unpublished).
[12] J.-L. Thomas, P. Roux, and M. Fink, ''Inverse scattering analysis with an acoustic time-reversal mirror,'' Phys. Rev. Lett. **72**, 637 (1994).
[13] S. R. de Groot, *Thermodynamics of Irreversible Processes* (North–Holland, Amsterdam, 1952).
[14] E. G. Flekkøy, ''Lattice BGK models for miscible fluids,'' Phys. Rev. E **47**, 4247 (1993).
[15] E. G. Flekkøy, U. Oxaal, J. Feder, and T. Jøssang, ''Hydrodynamic dispersion at stagnation points: Experiments and simulations,'' Phys. Rev. E **52**, 4952 (1995).
[16] A. M. Gurney, in *Fluorescent and Luminescent Probes for Biological Activity*, edited by W. T. Watson (Academic, London, 1992), p. 335.